Journal of Molecular and Cellular Cardiology 100 (2016) 83–92

Contents lists available at ScienceDirect

Journal of Molecular and Cellular Cardiology

journal homepage: www.elsevier.com/locate/yjmcc

Vascular action of bisphosphonates: In vitro effect of alendronate on the regulation of cellular events involved in vessel pathogenesis

Pablo H. Cutini, María B. Rauschemberger, Marisa J. Sandoval, Virginia L. Massheimer *

Instituto de Ciencias Biológicas y Biomédicas del Sur (INBIOSUR), Universidad Nacional del Sur (UNS), Consejo Nacional de Investigaciones Científicas y Técnicas (CONICET), Departamento de Biología, Bioquímica y Farmacia, San Juan 670, B8000ICN, Bahía Blanca, Argentina

ARTICLE INFO

Article history:
Received 27 June 2016
Received in revised form 19 August 2016
Accepted 24 August 2016
Available online 2 October 2016

Keywords:
Nitric oxide
Alendronate
Endothelial monocyte adhesion
Platelet adhesion and aggregation
Vascular calcification
Osteogenic markers

ABSTRACT

In this work we investigate whether, despite the procalcific action of alendronate on bone, the drug would be able to regulate in vitro the main cellular events that take part in atherosclerotic lesion generation. Using endothelial cell cultures we showed that Alendronate (1–50 μM) acutely enhances nitric oxide production (10–30 min). This stimulatory action of the bisphosphonate involves the participation of MAPK signaling transduction pathway. Under inflammatory stress, the drug reduces monocytes and platelets interactions with endothelial cells induced by lipopolysaccharide. Indeed the bisphophonate exhibits a significant inhibition of endothelial dependent platelet aggregation. The molecular mechanism of alendronate (ALN) on leukocyte adhesion depends on the regulation of the expression of cell adhesion related genes (VCAM-1; ICAM-1); meanwhile the antiplatelet activity is associated with the effect of the drug on nitric oxide production. On vascular smooth muscle cells, the drug exhibits ability to decrease osteogenic transdifferentiation and extracellular matrix mineralization. When vascular smooth muscle cells were cultured in osteogenic medium for 21 days, they exhibited an upregulation of calcification markers (RUNX2 and TNAP), high alkaline phosphatase activity and a great amount of mineralization nodules. ALN treatment significantly down-regulates mRNA levels of osteoblasts markers; diminishes alkaline phosphatase activity and reduces the extracellular calcium deposition. The effect of ALN on vascular cells differs from its own bone action. On calvarial osteoblasts ALN induces cell proliferation, enhances alkaline phosphatase activity, and increases mineralization, but does not affect nitric oxide synthesis. Our results support the hypothesis that ALN is an active drug at vascular level that regulates key processes involved in vascular pathogenesis through a direct action on vessel cells.

1. Introduction

Osteoporosis and cardiovascular disease (CVD) are multifactorial clinical entities that often coexist in postmenopausal women. Osteoporotic fractures, coronary and peripheral artery disease and stroke resulting from atherosclerosis, are common conditions particularly in the elderly. Epidemiological and clinical studies have shown an interesting relationship between osteoporosis and CVD mortality [1,2]. Disorders in bone metabolism and reduced bone mineral density reversely correlate with vascular calcification and this link is thought to contribute to high CVD mortality [3]. However, although these diseases have been traditionally considered as independent processes associated with age and ovarian status, increasing evidence confirms that both entities share pathophysiological mechanisms [2].

Bisphosphonates (BPs) are the most widely used category of therapeutic agents in osteoporosis [4]. These drugs are synthetic analogues of pyrophosphate in which the two phosphates are connected by an atom of carbon instead of oxygen. The presence of a nitrogen atom in the side chain [alendronate (ALN), pamidronate, ibandronate, risedronate, zoledronate] enhances their affinity for bone tissue. Traditionally, the bone protective effects of BPs have been attributed to induce osteoclasts apoptosis leading to decrease bone resorption. However, it has been recently reported that they also act directly on osteoblasts and osteocytes, to preserve their viability and to prolong their life span [5]. BPs have also been approved for the treatment of cancer-related skeletal complications, bone metastases, pain, nerve compression and fractures. Long bones are the most common site of spread to tumours such as breast, prostate, kidney and haematological cancers. The antineoplastic action induced by BPs involves disruption of intracellular vesicle transport, which reduces the ability of the cells to migrate and invade surrounding tissue [6]. Meanwhile, the proposed mechanisms for the beneficial effect of the BPs against hypercalcemia bone

* Corresponding author at: Cátedra de Bioquímica Clínica II, Departamento de Biología, Bioquímica y Farmacia, Universidad Nacional del Sur, San Juan 670, B8000ICN, Bahía Blanca, Argentina.
E-mail addresses: pcutini@uns.edu.ar (P.H. Cutini), mbrausch@criba.edu.ar (M.B. Rauschemberger), msandova@criba.edu.ar (M.J. Sandoval), massheim@uns.edu.ar (V.L. Massheimer).

http://dx.doi.org/10.1016/j.yjmcc.2016.08.017
0022-2828/

pain include inhibition of bone resorption, mechanical stabilisation, and enhancement of pH of the bone turnover microenvironment which results in decreased acid-sensing ion channel stimulation [7].

In concern with vascular action of BPs, existing data mostly belongs from clinical trials carried out in patients with chronic kidney disease and diabetes, where it is proposed that BPs could reduce the thickening of arterial vessels, and inhibit vascular calcification [8,9]. Although BPs seem to have an inhibitory effect on atherosclerosis process, the results are conflicting and it is not comprehensible whether the BPs act directly on vascular cells or indirectly through their action on bone system [10].

Atherosclerosis is a chronic inflammatory disease characterized by loss of vascular architecture, vascular injury (atheromatous generation), and finally, occlusion of the affected blood vessels [11]. The process starts with endothelial dysfunction, an event characterized by imbalance in the production of vasodilator and vasoconstrictor factors, followed by a marked decrease in the bioavailability of nitric oxide (NO) which leads to a pro-oxidant, proinflammatory and prothrombotic features [12]. The initial response to vascular injury is mediated by an increase of endothelial permeability and inflammatory cytokine secretion that consequently causes platelet adhesion to the activated endothelium. In turn, activated platelets promote the recruitment of monocytes, enhancing their transendothelial migration, and macrophage activation. The later stage of atherosclerotic lesion involves vascular tissue replacement by osteogenic like cells, extracellular matrix mineralization and intima calcification. This occurs as result of osteogenic transdifferentiation of vascular cells induced by the inflammatory microenvironment. Approximately 15% of human atherosclerotic plaques exhibit full calcification, with histological structure almost indistinguishable from bone trabecular architecture.

Bone mineralization and vascular calcification are cell-mediated processes sharing common mechanisms. The idea that pharmacological agents that inhibit bone loss could also provide benefits in terms of slowing the progression of atherosclerosis have grown up in the last years. The aim of the present work was to evaluate whether, despite the procalcific action of ALN on bone, the drug would be able to regulate in vitro the main cellular events that take part in atherosclerotic lesion generation. The direct effect of ALN either on endothelial cells (EC) and vascular smooth muscle cells (VSMC) was evaluated.

2. Materials and methods

2.1. Materials

Griess reagents were purchased from Britania Laboratories (Buenos Aires, Argentina). Trypsin/EDTA (10×), L-glutamine (100×), amphotericin B (0.25 mg/mL), penicillin/streptomycin (100×), and fetal calf serum (FCS) were obtained from PAA Laboratories (Pasching, Austria). Dulbecco's modified Eagle's medium (DMEM), ALN, and all other reagents were purchased from Sigma Chemical Company (St Louis, MO, USA).

2.2. Cell cultures and in vitro calcification

EC and VSMC cultures were obtained from aortic rings explants isolated from young Wistar rats (3–5 weeks old) as previously described [13]. Briefly, animals were killed by cervical dislocation and the full length thoracic aorta was aseptically removed. Immediately after, the aorta was cleaned of adherent connective tissue, and cut into small ring-shaped segments. Ring explants were seeded on 60-mm matrix-coated petri dishes containing phenol red-free DMEM supplemented with 20% (*v*/v) FCS, 60 μg/mL penicillin, 10 μg/mL streptomycin, 2.5 μg/mL amphotericin-B, 2 mM L-glutamine, and 1.7 g/L sodium bicarbonate. Explants were incubated at 37 °C in 5% CO_2 atmosphere. In order to establish a pure EC culture, after 5 days of culture, ring explants were removed and transferred into new culture dishes with fresh DMEM supplemented with 10% (*v*/v) FCS. Additional transfer of the ring explants resulted in pure cultures of VSMC. At last, the rings were discarded and EC and VSMC cultures were allowed to reach confluence. EC and VSMC identity was performed as previously reported (Supplementary Data) [13–15]. Cells from passages 2 to 5 were used for all experiments. Fresh medium containing 10% (*v*/v) FCS was replaced every 72 h. To perform cellular treatments ALN were dissolved in phosphate buffered saline (PBS) as vehicle.

In order to induce VSMC osteogenic differentiation, VSMC were seeded into 24-well plates and cultured for 21 days in DMEM containing 4 mM $CaCl_2$ and 10 mM β-glycerophosphate and 50 μg/mL ascorbic acid (osteogenic medium), as described [16]. The osteogenic medium was replaced by fresh medium every 3 days. The cells were exposed to the bisphosphonate (BP) or vehicle (control) in the last 24 h of culture. All the procedures were performed in accordance with the guidelines published in the *National Institutes of Health Guide for the Care and Use of Laboratory Animals*. All procedures involving animals and their care were performed at the Unit of Animal Care belonging to the Biology, Biochemistry and Pharmacy Department of the University. The Animal Care Use Committee of this Unit approved the protocol employed.

2.3. Osteoblast isolation and culture

Calvaria osteoblasts were obtained from 5-day-old neonatal rats as described by Santillán et al. [17]. Briefly, calvarias were incubated at 37 °C in PBS containing 4 mM EDTA for 10 min (two periods). The cultures medium were discarded. Subsequently, calvarias were rinsed in PBS and submitted to digestion in PBS containing 200 IU/mL collagenase for 15 min (four periods). Cells released during the first digestion were discarded, and those released during the subsequent digestions were spun down and collected after centrifugation (10 min at 1500 rpm). Then, cells were cultured at 37 °C in 5% CO_2 atmosphere in DMEM supplemented with 15% FCS, 2.15 g/L β-glycerophosphate, and 0.05 g/L ascorbic acid, 60 μg/mL penicillin, and 10 μg/mL streptomycin. After 24 h, the medium was replaced by fresh DMEM containing 10% FCS, and cells were cultured until 80% of confluence.

2.4. Measurement of NO production

Cells were seeded on 24-multiwell culture plates at a density of 3.5×10^4 cells/well in DMEM containing 10% (*v*/v) FCS. Prior treatment, culture medium was changed by fresh DMEM containing 1% (v/v) FCS. In vitro treatments were performed by of ALN or vehicle (PBS) addition. When specific antagonist/inhibitors were used, they were added to culture medium 1 h before ALN treatment. Nitrites were measured in the incubation media as a stable and non-volatile breakdown product of the NO released, employing the spectrometric Griess reaction [14]. Briefly, once finished treatment, aliquots of culture medium supernatant were mixed with Griess reagent (1% sulphanilamide and 0.1% naphthylenediamine dihydrochloride in 2.5% phosphoric acid) and incubated 10 min at room temperature. Absorbance was measured at 548 nm in a microplate reader (Biotek Synergy-HT). Nitrite concentration in the samples was determined with reference to a sodium nitrite ($NaNO_2$) standard curve performed in the same matrix. Cells were dissolved in 1 M NaOH, and protein content was measured by Lowry method [18]. The results were expressed as nmol of NO per mg of protein. The quantification of NO production through the indirect method of Griess, was validated against direct measurements of nitric oxide synthase (NOS) activity using the ^{3}H–arginine to ^{3}H–citrulline conversion method [19]. Similar results were obtained with both assays.

2.5. Monocyte adhesion assay

2.5.1. Monocyte isolation

Peripheral blood mononuclear cells were obtained using density gradient (Ficoll-Paque Plus) and monocytes were isolated by adherence to plastic dishes as previously described [20]. Briefly, heparinized whole blood diluted with PBS (1:1) was carefully layered onto Ficoll-Paque

Plus and centrifuged at 400g. Mixed mononuclear cell interface was collected, and viability was checked with trypan blue. Peripheral blood mononuclear cell were suspended in DMEM-10% FCS and placed on Petri dishes (2×10^7 cells/mL) for 1 h at 37 °C to allow peripheral blood monocyte adhesion. Culture medium containing non-adherent cells was removed. Adhered cells were incubated for 15 min in PBS–EDTA 10 mM, washed and cultured in DMEM containing 10% FCS, 60 mg/mL penicillin, 100 mg/mL streptomycin for 72 h. Adherent cells were detached using a rubber policeman and suspended in DMEM. Absolute number of monocytes was counted using an automatized counter. Cell viability was confirmed by trypan blue assay.

2.5.2. Monocyte adhesion assay

EC were exposed to ALN treatment in the presence or absence of 1 μg/mL lipopolysaccharide (LPS). An exact number of monocytes was seeded on pre-treated EC and incubated for 2 h at 37 °C in a humidified 5% CO_2 atmosphere. Supernatants of each well containing non-adhered monocytes were collected and counted [20]. The number of adhered monocytes to EC was calculated by the difference between total mononuclear seeded and non-adhered monocytes. EC monolayer containing adhered monocytes were dyed using Giemsa staining. Images (400×) were obtained using a digital camera (Olympus C7070WZ) coupled to an optical microscope (Olympus BX51). Results are expressed as means and standard deviation (SD) of number of adhered monocytes/well.

2.6. Platelet assays

2.6.1. Platelet isolation

For platelet aggregation assays, rat platelet-rich plasma (PRP) was obtained as previously described [21]. For platelet adhesion assays, PRP was fixed in 4% (*v*/v) formaldehyde/PBS for 10 min, suspended in PBS (pH 7.4) at room temperature and centrifuged at 750 ×*g* for 10 min. Then, fixed platelets were washed twice with PBS. Platelet count was performed using a hemacytometer, and then, they were suspended at a final concentration of 5×10^6 platelets/mL in DMEM supplemented with 1% (*v*/v) FCS [22].

2.6.2. Platelet adhesion assay

EC were seeded on 24-multiwell culture plates and then exposed to ALN, LPS (1 μg/mL) or ALN plus LPS in DMEM supplemented with 1% (v/v) FCS. Once finished treatment, EC were washed twice with PBS, and 1.5×10^6 platelets/well were added on pre-treated cells. Platelets were allowed to adhere to EC for 2 h at 37 °C. Supernatants of each well containing non-adhered platelets were collected and counted employing a hemacytometer. The number of adhered platelets to EC was calculated by difference between total added platelets and non-adhered platelets. Results are expressed as mean ± SD of the number of adhered platelets/well [22].

2.6.3. Platelet aggregation assay

Platelet aggregation was measured using a turbidimetric assay as previously described [22]. EC were seeded on 24-multiwell culture plates at a density of 3×10^4 cells/well in DMEM supplemented with 10% (*v*/v) FCS. Culture medium was replaced by 400 μL of PRP (3×10^8 platelets/mL) and exposed to ALN or vehicle (control) for 10 min. Immediately after treatment, 285 μL of PRP were taken and set in a CronoLog 430 aggregometer cuvette with continuous stirring. Aggregation was initiated by addition of $2 \times 10–^5$ M adenosine diphosphate (ADP). Control group (EC in PRP) was treated with vehicle alone (PBS). Changes in light transmission were recorded for 5 min after ADP addition. EC were dissolved in 1 M NaOH and aliquots were taken for protein determination by Lowry method. Results were calculated as platelet aggregation/mg protein and expressed as percentage of inhibition of platelet aggregation with respect to control. When the direct effect of the BP on platelets was evaluated, PRP was incubated with ALN in the absence of EC, and platelet aggregation was measured as described above. Basal aggregation was considered the maximal aggregation exhibited by PRP alone. Results were expressed as percentages of platelet aggregation with respect to basal.

2.7. Alkaline phosphatase (ALP) activity assay

ALP activity of cell lysates was measured using a commercially available kit [16]. After treatment, cells were washed three times with PBS and lysed with 300 μL of 0.2% TritonX-100 (Sigma-Aldrich), 150 mM NaCl, 3 mM $NaHCO_3$ for 30 min at 37 °C. The culture medium was collected and stored at 4 °C until assay was performed. ALP activity was measured using p-nitro-phenyl phosphate as a substrate, according to manufacturer's instruction. Protein content was measured by Lowry method. Results are expressed as IU/mg protein.

2.8. Methyl thiazolyl tetrazolium (MTT) cell proliferation assay

Cell proliferation was evaluated by the MTT (3-(4,5-dimethylthiazolyl-2)-2, 5-diphenyltetrazolium bromide) conversion assay [23]. Cells were seeded into 96-multi-well plates in DMEM supplemented with 10% (*v*/v) FCS and allowed to grow up to 60–70% confluence. Cells were synchronized by placing in serum-free DMEM for 24 h, and further exposed to ALN or vehicle (control) in fresh DMEM containing 1% (v/v) FCS. After treatment, the medium was removed, and MTT solution (5 mg/mL) was added to each well followed by incubation for 4 h at 37 °C. Immediately after, the supernatant was carefully removed and the resulting intracellular formazan crystals were dissolved in dimethylsulfoxide, and the absorbance value was measured at 550 nm in a microplate reader (Biotek Synergy-HT). Optical density (OD) is directly proportional to number of proliferating cells.

2.9. Alizarin red staining

At 21 days of culture the presence of calcified nodules were analyzed by alizarin red staining [24]. Once finished treatment, cells were fixed in 4% paraformaldehyde for 10 min and subsequently washed three times with PBS. Cells were stained with 2% alizarin red solution for 30 min at room temperature and washed three times with distilled water to remove residual stain. The stained culture plates were photographed (Olympus C7070WZ).

2.10. Measurement of extracellular calcium deposition

Cells were decalcified with 0.6 mol/L HCl for 24 h, and calcium content in the supernatant was determined by spectrophotometry using the o-cresolphthalein complexone method (Wiener lab, Argentina). Following decalcification, cells were washed with PBS and solubilized with 1 mol/L NaOH and protein content was measured by Lowry Method. Cellular calcium levels were normalized to the total protein content and expressed as μg/mg protein.

2.11. Reverse transcription-polymerase chain reaction (RT-PCR) assay

Expression of the adhesion molecules, VCAM-1, ICAM-1, RUNX2 and TNAP was determined using the Superscript III CellsDirect cDNA synthesis system (Invitrogen, California, USA). In order to assess VCAM-1 and ICAM-1 expression, EC (grown in 12-well culture plates) were treated for 24 h with 10 μM ALN in the presence or absence of LPS (1 μg/mL), which was employed as adhesion molecule expression inductor. Cells were washed twice with ice-cold PBS and total cellular RNA extraction and RT-PCR were performed according to the manufacturer's instructions. Complementary DNA was amplified using a programmed Thermocycler (Biometra Uno II, Göttingen, Germany). PCR cycles were as follows: VCAM-1 (95 °C, 3 min, 95 °C, 60 s, 55 °C, 60 s, 72 °C, 60 s, 72 °C, 7 min, 32 cycles); ICAM-1 (95 °C, 3 min, 94 °C,

60 s, 64 °C, 60 s, 72 °C, 60 s, 72 °C, 7 min, 32 cycles). Primers sequences were: VCAM-1: forward: 5′-TAA GTT ACA CAG CAG TCA AAT GGA-3′, reverse: 5′-CAC ATA CAT AAA TGC CGG AAT CTT-3′; ICAM-1: forward: 5′-CTG CAG AGC ACA AAC AGC AGA G-3′, reverse: 5′-AAG GCC GCA GAG CAA AAG AAG C-3′ [20,25]. In order to assess RUNX2 and TNAP expression, VSMC and VSMC-OB (grown in 12-well culture plates) were treated for 24 h with vehicle (PBS) or 10 μM ALN and total cellular RNA extraction and RT-PCR were performed according to the manufacturer's instructions. PCR amplification steps were as follows: RUNX2 (95 °C, 3 min, 95 °C, 60 s, 60 °C, 60 s, 72 °C, 60 s, 72 °C, 7 min, 35 cycles); TNAP (95 °C, 3 min, 95 °C, 60 s, 63 °C, 60 s, 72 °C, 60 s, 72 °C, 7 min, 35 cycles). Primers sequences were: RUNX2: forward: 5′-GTT ATG AAA AAC CAA GTA GCC AGG T-3′, reverse: 5′-GTA ATC TGA CTC TGT CCT TGT GGA T-3′; TNAP: forward: 5′-TGG ACG GTG AAC GGG AGA AC-3′, reverse: 5′-TGA AGC AGG TGA GCC ATA GG-3′ [26,27]. The expression of housekeeping gene GAPDH (glycerldehyde-3-phosphate dehydrogenase) was checked for each set of RT-PCR experiments (forward primer: 5′-TCC CTC AAG ATT GTC AGC AA-3′, reverse primer: 5′-AGA TCC ACA ACG GAT ACA TT-3′. Amplification steps: 95 °C, 3 min, 94 °C, 30 s, 53 °C, 30 s, 72 °C, 45 s, 72 °C, 7 min, 35 cycles) [25]. Negative controls (PCR reaction without RT product) were also processed. PCR amplification products were detected by electrophoresis in agarose gels stained with ethidium bromide. The density of each band gel was quantified using ImageJ software (1.5e version, NIH, Rasband). Each sample was normalized against GAPDH. Results were obtained from at least 3 independent experiments.

2.12. Statistical analysis

The results presented were obtained from three independent experiments where each individual experimental condition was performed by quadruplicate ($n = 4$). All data are presented as mean ± SD. Different cell cultures were used for each independent experiment. Comparisons between two means were made using Student's *t*-test, and multiple comparisons with one or two ways ANOVA, followed by Fisher's Least Significant Difference Test, using SPSS Statistics 23.0 software for Windows. *P*-values lower than 0.05 were considered to be statistically significant.

3. Results

3.1. Effect of ALN on NO production by EC

Fig. 1A shows that, in EC, ALN induced a significantly increase on NO production early at 10 min of treatment (38–104% above control, 1–50 μM ALN, $p < 0.02$). Stimulatory action was sustained towards 30 min of in vitro exposure to the BP. The effect was detected in a dose range of 1–50 μM. Lower concentrations (0,001–100 nM) did not affect vasoactive production (data not shown). The levels of NO production induced by ALN were lower than that induced by acetylcholine (Ach), a physiological vasoactive that stimulates NOS activity in endothelium (503 ± 65 vs 188 ± 19, 100 μM ACh vs control, $p < 0.001$). Since MAPK and PKC pathways are signal transduction systems commonly involved in vascular physiology [28,29], using specific kinase antagonists we checked the participation of these signaling cascades on BP action (Fig. 1B). The involvement of MAPK transduction system was assessed using a MEK inhibitor, the compound PD98059. When EC cultures were preincubated 1 h with 5 μM PD98059 prior to ALN treatment, the enhancement on NO production induced by the BP was completely suppressed. Meanwhile, the preincubation of EC with chelerythrine (Chel), a PKC inhibitor, did not affect the stimulatory action of ALN on NO production. The reversal of the stimulatory effect of ALN by the presence of the NOS inhibitor N-nitro-L-arginine methyl ester (L-NAME), proved the specificity of NO measurements (Fig. 1B).

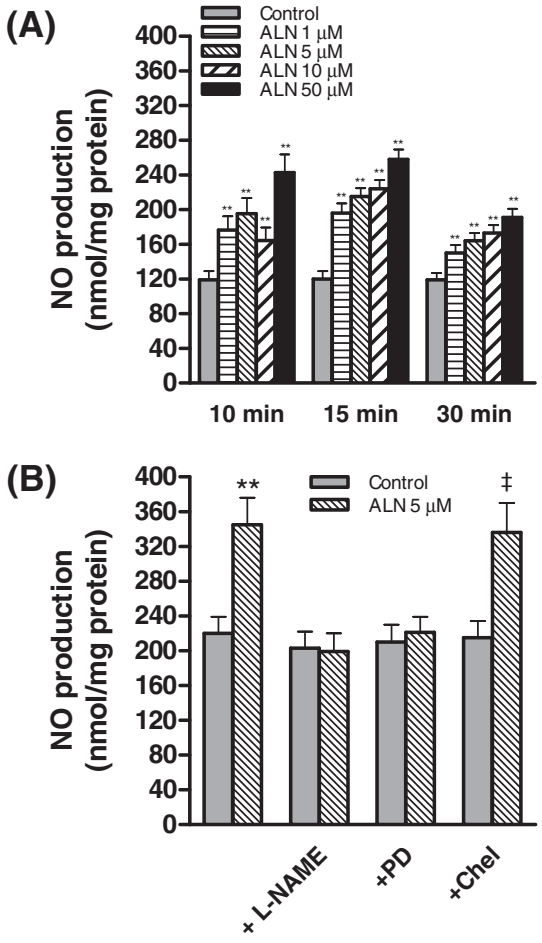

Fig. 1. Effect of MAPK and PKC inhibitors on the stimulation of NO production induced by ALN. NO production was measured by Griess reaction as described in Materials and methods section. Results represent the average ± SD of three independent experiments ($n = 4$). (A) EC were treated with different concentrations of ALN at the indicated times. $^{**}p < 0.02$ vs each control. (B) EC were pre-incubated 1 h in the absence or presence of 10 μM L-NAME, 5 μM PD98059 (PD) or 1 μM chelerythrine (Chel), and then exposed to 5 μM ALN for 10 min. $^{**}p < 0.02$ vs control without inhibitor; ‡$p < 0.02$ vs control with Chel.

3.2. Modulation of monocyte–EC interaction by ALN

Using cell adhesion assay, we evaluated the effect of ALN on monocyte–EC interaction. EC were treated with 5 μM ALN or vehicle alone for 24 h in presence or absence of the proinflammatory agent LPS (1 μg/mL). Immediately after, peripheral blood monocytes were added and allowed to seed for additional 2 h. Fig. 2B shows that, BP treatment had no effect on basal monocyte–EC adhesion. As can be expected, LPS markedly enhanced monocyte adhesion. However, when EC were incubated with ALN prior to LPS addition, the enhancement of monocyte adhesion induced by LPS was partially reduced (25% reduction of leukocyte adhesion, $p < 0.05$). Fig. 2A also shows representative microphotographs of each experimental condition.

Since monocyte adhesion to EC depends on the expression of surface adhesion molecules such as ICAM-1 and VCAM-1, using RT-PCR technique we checked the effect of ALN on the regulation of mRNA expression of these molecules. Fig. 2C-D shows that, in EC, LPS treatment markedly enhanced mRNA expression of both molecules compared to control group. When ALN was added before LPS, the mRNA levels were significantly down regulated.

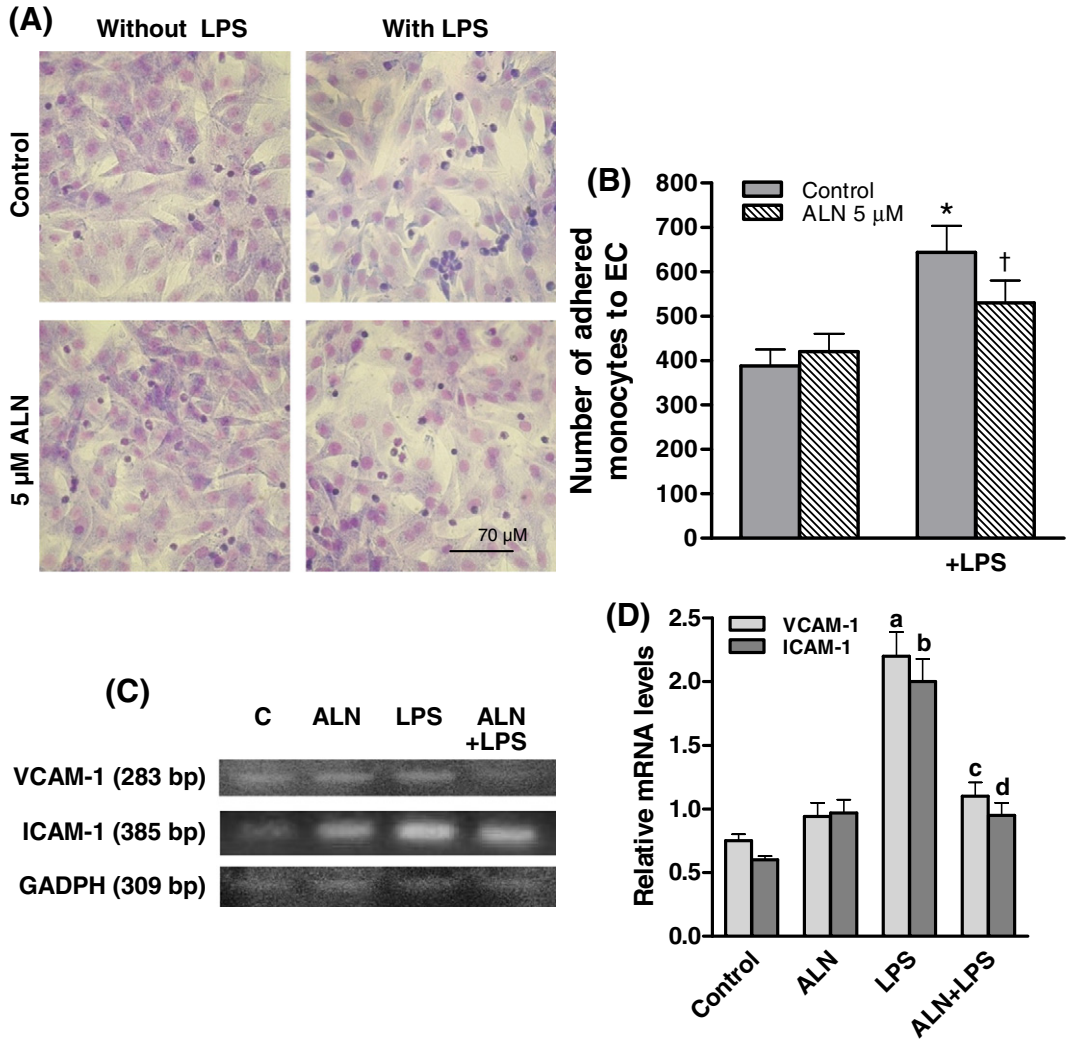

Fig. 2. Effect of ALN on monocyte adhesion. EC cultures were treated with 5 µM ALN or vehicle alone (control) for 24 h in the absence or presence of 1 µg/mL LPS, which was added during the last 21 h of BP treatment. Monocytes adhesion to EC was performed as described under methods. (A) Cells were stained using Giemsa solution. Images show representative fields of each experimental condition (×400). The scale bar represents 70 µm. (B) Monocytes were counted as described in methods. Bars represent the means ± SD of three independent experiments ($n = 4$). *$p < 0.05$ vs control without LPS; †$p < 0.05$ vs LPS. (C) mRNA expression of EC adhesion molecules VCAM-1 and ICAM-1performed by RT-PCR as described in methods. Representative gel photography of PCR amplification products is shown. (D) Bars show the relative intensity of each band determined by densitometric analysis. Data are presented as VCAM-1 and ICAM-1 mRNA relative to GADPH mRNA, and are the average ± SD of three independent experiments ($n = 4$). $^{a,b}p < 0.05$ vs control; $^{c,d}p < 0.05$ vs LPS.

3.3. Regulation of platelet–EC interaction by ALN

In order to study the effect of the BP on platelet–EC interaction, platelet adhesion and platelet aggregation were evaluated. EC monolayers were treated with 1, 5, or 10 µM ALN during 24 h in the presence or absence of LPS. Immediately after, platelets were seeded on EC monolayers for 2 h. Under basal conditions, ALN partially reduced the number of platelets adhered to EC throughout all range of concentrations tested (Fig. 3, left side). When EC were incubated in a proinflammatory microenvironment (presence of LPS), platelet adhesion was significantly enhanced (34% above control, $p < 0.02$). Similarly as in monocyte adhesion assays, the enhancement in platelet adhesion induced by LPS was partially reduced by the presence of ALN (22–33% of reduction; 1–10 µM ALN, $p < 0.02$). Since vascular NO bioavailability is a key regulator of platelet–EC interactions, we checked whether the inhibition by ALN of the LPS induced platelet adhesion could depend on the ability of the drug to stimulate endothelial NO production. As can be observed in Table 1, the presence of L-NAME significantly reduced the inhibitory action of the BP on the induction of platelet adhesion elicited by the inflammatory agent.

Afterwards, the effect of ALN on platelet aggregation was studied. EC were incubated with PRP and subsequently exposed to different concentrations of the BP (0.1 and 10 µM) for 10 min. Table 2 shows the quantitative data obtained. ALN significantly inhibited platelet aggregation compared to control cells (39 and 56% inhibition). Once more, in the presence of L-NAME, the antiaggregatory action of ALN was blunted (Table 2). A direct action of the BP on platelets was ruled out, since when platelet aggregation was measured in the absence of EC, maximal aggregation was detected still in the presence of ALN. Altogether, these results suggest that ALN modulates platelet adhesion and aggregation in a NO dependent manner.

3.4. Effect of ALN on vascular cells proliferation

Since alterations in vascular cell proliferation patterns are also implicated in atherosclerosis, the effect of ALN on vascular cell growth was evaluated. Our results show that the temporal profile of vascular cells proliferation was not mainly modified by ALN (Fig. 4). Only a 0.5 fold increase in VSMC proliferation was observed after 24 h of ALN treatment

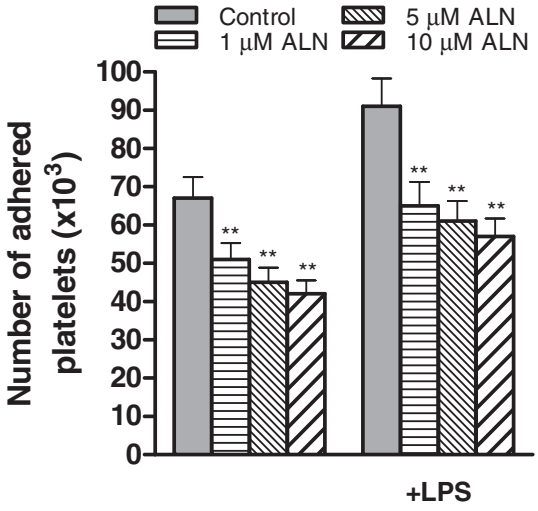

Fig. 3. Effect of ALN on platelet adhesion. EC cultures were treated with ALN at the indicated concentrations for 24 h in the presence or absence of 1 μg/mL LPS, which was added during the last 21 h of BP treatment. Platelets were seeded on EC monolayer and were counted as described in methods. Results are the average ± SD of three independent experiments (n = 4). $^{**}p < 0.02$ respective to each control.

(Fig. 4, right panel). Similar results were obtained when proliferation was quantified by cell number counting (data not shown).

3.5. ALN and VSMC osteogenic transdifferentiation

To explore the effect of ALN treatment on smooth muscle cells, monolayers were incubated for 21 days in osteogenic medium. As features of muscle cell transdifferentiation (VSMC-OB) the expression of calcification markers; ALP activity and the presence of calcified nodules were analyzed. Fig. 5A shows that VSMC-OB exhibited a 4 fold increase in ALP activity compared to native VSMC. When mineralized muscle cells were exposed to ALN treatment, ALP activity was significantly reduced. Basal activity of ALP was not modified by the osteogenic medium.

Indeed, extracellular calcium deposition (evidenced by alizarin staining and by quantification of HCl leaching of calcium), was markedly enhanced in VSMC-OB respect to native cells. After ALN treatment, the presence of calcified nodules in VSMC-OB was diminished (Fig. 5B and C).

Fig. 5D shows the quantification of mRNA levels of the calcification markers RUNX2 (Runt-related transcription factor 2) and TNAP (tissue non-specific alkaline phosphatase). As can be observed, both markers were detected in VSMC-OB but not in native cells. After 12 h treatment of the transdifferentiated cells with 10 μM ALN, the expression of the calcification markers was down-regulated.

Table 1
Inhibition by ALN of LPS-induced platelet adhesion: effect of L-NAME.

Treatment	Percentage of inhibition of LPS-platelet induced adhesion[a]	
	Without L-NAME	With L-NAME
1 μM ALN	28,12 ± 3,02[†]	2,34 ± 0,35[#]
5 μM ALN	30,58 ± 2,94[†]	0,51 ± 0,46[#]
10 μM ALN	35,27 ± 3,42[†]	15,65 ± 1,15[#]

[#] P < 0.02 vs LPS.
[†] P < 0.02 vs LPS.
[a] EC cultures were treated with ALN or vehicle (control) at the indicated concentrations for 24 h in the presence of 1 μg/mL LPS, which was added during the last 21 h of BP treatment. When the NOS inhibitor L-NAME (10 μM) was employed it was added 1 h before treatment. Platelets were seeded on EC monolayer and were counted as described in Materials and methods section. Results are the average ± SD of three independent experiments ($n = 4$).

Table 2
Effect of ALN on platelet aggregation.

Treatment	Percentage of inhibition of platelet aggregation with respect to control[a]	Percentage of platelet aggregation with respect to basal[b]
0.1 μM ALN	38.9 ± 4.3[*]	97.3 ± 8.2
10 μM ALN	56.8 ± 5.5[**]	97.6 ± 8.1
0.1 μM ALN + L-NAME	4.5 ± 0.3[†]	98.4 ± 7.5
10 μM ALN + L-NAME	5.1 ± 0.4[†]	98.2 ± 6.8

[*] $P < 0.05$ vs control.
[**] $P < 0.02$.
[†] $P < 0.05$ with respect to corresponding ALN treatment without L-NAME.
[a] EC monolayers were incubated in PRP with ALN (0.1–10 μM) or vehicle (control) for 10 min. PRP was quickly removed and platelet aggregation was measured as described in Material and methods section. When the NOS inhibitor L-NAME (10 μM) was employed, EC were preincubated for 30 min before treatment. Results are expressed as percentage of inhibition of platelet aggregation with respect to control group (100%) and are the average ± S.D. of three independent experiments ($n = 4$).
[b] Aliquots of PRP were incubated with ALN (0.1–10 μM) in the absence of EC for 10 min. Basal group received vehicle alone. Immediately after ADP was added, platelet aggregation was measured. Results are expressed as percentage with respect to basal aggregation (100%) and represent the average ± S.D. of three independent experiments ($n = 4$).

3.6. Effect of ALN on calvaria osteoblastic cells

As control of ALN bone action, we tested the effect of the BP on calvaria osteoblastic cells. ALN markedly enhanced osteoblastic ALP activity (135–338% above control, 0.01–10 μM respectively), and stimulated cell proliferation (Fig. 6A). Indeed, ALN treatment increase extracellular calcium deposition (766 ± 77 vs 519 ± 32 μg calcium/mg protein, 10 μM ALN vs control, $p < 0.01$). However, when the effect of the BP on bone NO synthesis was tested, in contrast with the stimulatory action of ALN on EC, the BP did not affect osteoblastic NO production (Fig. 6B).

4. Discussion

In this work we provide evidence of a possible beneficial action of BP on vascular homeostasis. A direct action either on endothelial and on smooth muscle vascular cells was demonstrated. The drug acutely enhances endothelial NO production, and under inflammatory stress reduces monocytes and platelets interactions with EC. The molecular mechanism shows that the effect of ALN on leukocyte adhesion depends on the regulation of expression of cell adhesion related genes; meanwhile the antiplatelet activity is associated with the effect of the drug on the vasoactive production. On VSMC, the drug exhibits ability to decrease osteogenic transfifferentiation. A significant reduction on the expression of osteoblasts markers and on extracellular matrix mineralization was observed after ALN exposure. The effect of ALN on vascular cells differs of its own bone action. On calvarial osteoblasts ALN induces cell proliferation, enhances ALP activity, and increases mineralization, but do not affected NO synthesis.

Among literature, it is largely unknown which are the ALN levels reached in the bone microenvironment under therapeutic treatments. The concentration range of BP tested in this study was selected from in vitro studies involving osteoblastic [30] or EC [31].

There is substantial evidence in the literature about the role of NO production on the regulation of vascular tone and homeostasis. Endothelial NOS (eNOS) activity is fast regulated by transient changes in intracellular calcium and phosphorylation through several intracellular transduction cascades (PI3K/AKT, AC/PKA, CaMKII, PLC/PKC, and MAPK) [32]. Endothelial NO bioavailability can be modified by a plethora of hormones and factors [33]. Here, we showed that endothelial NO generation could be also modulated by ALN. The drug elicits a rapid and significant stimulation of NO production that involves the participation of MAPK transduction system. The time course of ALN treatment tested is in accordance with the short time interval required

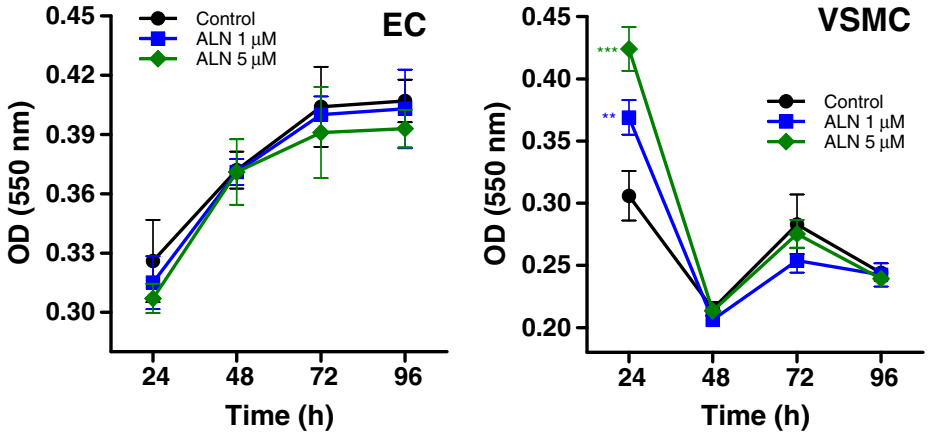

Fig. 4. Effect of ALN on EC and VSMC proliferation. EC and VSMC were treated with ALN at the indicated concentrations for 24, 48, 72 or 96 h. Cell proliferation was measured by MTT assay as described in methods. Results represent the average ± SD of three independent experiments (n = 4). $^{**}p < 0.02$ and $^{***}p < 0.001$ vs control (24 h).

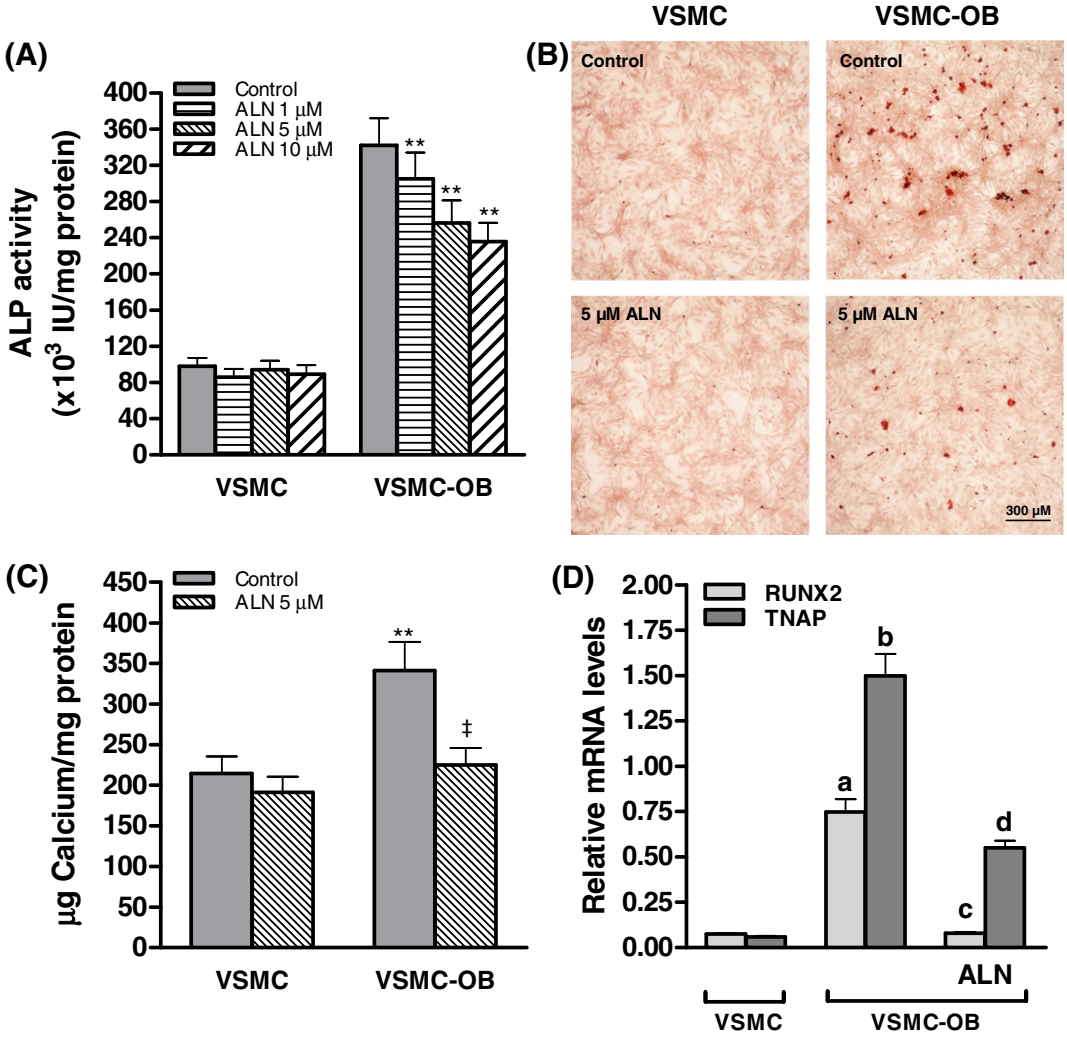

Fig. 5. Effect of ALN on VSMC osteogenic transdifferentation. Cells were cultured 21 days in normal medium (VSMC) or osteogenic medium containing 4 mM $CaCl_2$ and 10 mM β-glycerophosphate (VSMC-OB). ALN was added at the indicated concentrations during the last 24 h of incubation period. Results represent the average ± SD of three independent experiments (n = 4). (A) ALP activity was measured as described in methods. $^{**}p < 0.02$ vs VSMC-OB control group. (B) Images show representative fields of Alizarin staining. Scale bar = 300 μm. (C) Measurement of calcium deposition performed as described methods. $^{**}p < 0.02$ vs VSMC control group; $^{‡}p < 0.02$ vs VSMC –OB control group. (D) Quantification of mRNA expression of the calcification markers of RUNX2 and TNAP. mRNAs were isolated from VSMC or VSMC-OB exposed to 5 μM ALN or vehicle alone for 12 h. RT-PCR was performed as described methods, and PCR amplification products were analyzed by electrophoresis. Bars represent the relative intensity of each band normalized against GADPH mRNA determined by densitometric analysis, and are the average ± SD of three independent experiments (n = 4). $^{a,b}p < 0.05$ vs VSMC; $^{c,d}p < 0.05$ vs VSMC-OB control group.

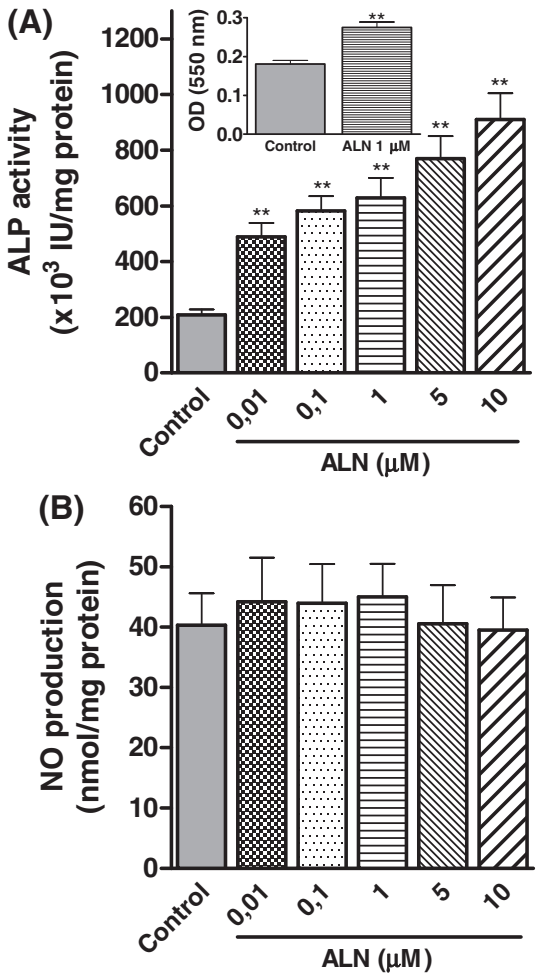

Fig. 6. Effect of ALN on calvarial osteoblasts. (A) Calvaria cells were treated with vehicle (PBS) or ALN at the indicated concentrations for 24 h and ALP activity was measured as described in methods. Insert: calvaria cells were treated with 1 μM ALN for 24 h and cell proliferation was measured by MTT assay as described in methods. $^{**}p < 0.02$ vs control. (B) Calvaria cells were treated with vehicle (PBS) or ALN at the indicated concentrations for 10 min and NO production was measured as described in methods. Results represent the average ± SD of three independent experiments (n = 4).

to eNOS stimulation. It has been reported that, in bone marrow stromal cells ALN stimulates osteoblatogenesis and inhibits adipogenic differentiation, through MAPK pathway activation [34]. The relationship between BPs and NO synthesis depends on the experimental systems employed, and/or the isoform of NOS involved. In gastric cells, it has been reported that ALN reduces NO production, which was associated with gastric ulcerogenic response and mucosa damage induced by BP treatment [35]. In macrophages cell lines, aminobisphophonates like ALN had no effect on NO production [36], meanwhile in chondrocytes pamidronate and other aminobisphophonates exhibit anti-inflammatory protective effects by reducing the enhancement in inducible NO activity elicited by TNF-α [37]. The impact of ALN on endothelial NO production could benefit not only vessel walls, but also bone tissue. After synthesis, NO would be released to vascular lumen. The vasoactive appears to play an important regulatory role on bone metabolism, stimulates osteoblast proliferation, osteocalcin synthesis and in vitro formation of mineralized matrix, and keeps the osteoclast mediated bone resorption under control [38]. Indeed NO can also facilitate fracture healing, and promote mechanical stress bone formation [39]. NO may also be synthethized in bone cells. However our results showed that, in OB, ALN do not affect NO production as it does in EC.

In healthy conditions, the endothelium remains in a nonactivated state. The initial response to vascular injury includes activation, adhesion and aggregation of platelets to endothelium. We demonstrated that, under inflammatory stress, ALN treatment prevents the adhesion of platelets or monocytes to activated EC. These data would suggest a vasoprotective role of the drug against vascular inflammation. The molecular mechanism displayed by the drug shows of a link between NO and platelet endothelium interaction and, a regulatory effect on cell adhesion molecules (CAMs) transcription. The ability of the BP to inhibit platelet adhesion and aggregation depends on its direct action on EC increasing NO liberation. Additionally the BP attenuates the LPS induced expression of endothelial cell surface molecules involved in leukocyte adhesion (ICAM-1; VCAM-1).

On cell growth our results show that, at vascular level, ALN does not affect cell proliferation in contrast to the proliferative effect elicited on osteoblasts. It is known that vascular cell growth and migration are involved in angiogenesis. Evidence in the literature demonstrate that nitrogen-containing BPs exhibit antiangiogenic properties due to their ability to inhibit several steps involved in angiogenesis such as EC proliferation, adhesion and migration, reduce capillary like tube formation, and prompt EC apoptosis [40]. However, the evidence of antiangiogenic properties of BPs may also cause poor wound healing [41], and osteonecrosis of the jaws. The latter has been primarily attributed to suppression of bone turnover due to BPs induced inhibition of osteoclasts activity, together with conditions that are unique to the mandible and maxilla. These provoke a hypodynamic bone unable to respond to repair processes associated with physiologic trauma or infection. It has been reported that zoledronate inhibits proliferation and migration of VSMC. These findings were strongly associated with vasoprotective effects of BPs reducing neointimal hyperplasia and atherosclerosis disease progression [42]. The authors showed that, low concentrations of BP do not alter vascular muscle cells growth; meanwhile high concentrations (100 μM) significantly inhibit VSMC proliferation.

Atherosclerosis calcification may occur as a consequence of plaque progression. Although vascular calcification was once thought to be a passive physico-chemical event of extracellular mineralization, in the last two decades a great body of evidence shows that it is an active cellular pathobiological process where inflammation, macrophages and VSMC play a crucial role [43]. One of the main cellular events of vessel skeletonized is the osteogenic transdifferentiation of VSMC [44]. The biomineralization of the vascular muscle cells is associated with up-regulation of calcification genes such as RUNX2, BMP-2 (bone morphogenetic protein-2), the sodium-dependent phosphate cotransporter Pit-1; and TNAP. Under physiological conditions TNAP is not expressed in arterial muscle cells, and its induction means irreversible modification towards mineralization by decreasing inorganic pyrophosphate levels [45]. After 21 days of culture in calcification media, we showed that VSMC exhibit an upregulation of calcification markers, posses high ALP activity, and also exhibit a great amount of mineralization nodules. Our evidence demonstrated that, ALN in vitro treatment partially reduces VSMC-OB transdifferentiation by diminishing RUNX2 and TNAP mRNA levels, and reducing ALP activity and extracellular calcium deposition. In agreement with our observations, similar doses of ALN inhibit bovine vascular smooth muscle cell calcification through restoring the expression of matrix Gla protein, a potent inhibitor of vascular calcification [46]. Indeed, in a rat model of vascular injury, nanosupenssions of ALN reduced neointimal hyperplasia and stenosis [47].

In order to check ALN bioactivity, we evaluated the effect of the drug on bone. In accordance with previous reports [5], our results show that ALN enhances OB proliferation, enhances ALP activity, and increases extracellular calcium deposition.

In this work, several insights of the molecular mechanism of action of alendronate on vascular wall have been outlined. However, the complete elucidation, step-by-step, of the pathway by which the BPs acts remains unknown. Further investigations will be carried out in order to fully comprehend the signaling transduction cascades involved in alendronate vascular action.

Over the past two decades preclinical and clinical studies performed reinforced and highlighted the critical importance of bone-vascular interactions. The vasculature provides the conduit for osteoprogenitor invasion and, for mineral exchange. Dual selective actions of BPs on vascular and bone have been recently reported [9,48]. It remains unknown, whether medical strategies for osteoporosis would simultaneously reduce initiation and progression of vascular disease.

5. Conclusions

Our results support the hypothesis that ALN is an active drug at vascular level that regulates key processes involved in vascular pathogenesis, through a direct action on vessel cells. The drug affects cellular and molecular events involved in the earlier and advanced stage of atherosclerosis disease. On the former, the BP actions include the regulation of monocyte and platelet adhesion to EC; the bioavailability of NO, and the expression of CAMs. On the late stage, the drug attenuates osteogenic transdifferentiation of VSMC by reducing expression of osteoblastic bone markers and extracellular mineralization. The effect on VSMC represents an opposite effect compared with the action of the drug displayed on osteoblasts.

Due to the relevant cellular events affected by ALN action, and since the data obtained belongs from in vitro assays with isolated cells, the results must be extrapolated in an animal model. As stated above, healthy vessels are essential for bone growth and remodeling. Whether ALN could be used as a drug with dual purpose remains unclear, and further studies should be undertaken to elucidate this matter.

Disclosures

None.

Acknowledgments

The authors would like to thank Graciela Santillán, PhD from Departamento de Biología, Bioquímica y Farmacia, Universidad Nacional del Sur, Bahía Blanca, Argentina, for kindly providing calvaria cells. This research was supported by grants from the SGCyT, Universidad Nacional del Sur, Bahía Blanca, Argentina (PGI 24/B203); Consejo Nacional de Investigaciones Científicas y Técnicas (CONICET, Argentina, PIP D-4061).

Appendix A. Supplementary data

Supplementary data to this article can be found online at http://dx.doi.org/10.1016/j.yjmcc.2016.08.017.

References

[1] L.B. Tanko, C. Christiansen, D.A. Cox, M.J. Geiger, M.A. McNabb, S.R. Cummings, Relationship between osteoporosis and cardiovascular disease in postmenopausal women, J. Bone Miner. Res. 20 (2005) 1912–1920.
[2] S.I. McFarlane, R. Muniyappa, J.J. Shin, G. Bahtiyar, J.R. Sowers, Osteoporosis and cardiovascular disease: brittle bones and boned arteries, is there a link? Endocrine 23 (2004) 1–10.
[3] P. von der Recke, M.A. Hansen, C. Hassager, The association between low bone mass at the menopause and cardiovascular mortality, Am. J. Med. 106 (1999) 273–278.
[4] I.R. Reid, Short-term and long-term effects of osteoporosis therapies, Nat. Rev. Endocrinol. 11 (2015) 418–428.
[5] T. Bellido, L.I. Plotkin, Novel actions of bisphosphonates in bone: preservation of osteoblast and osteocyte viability, Bone 49 (2011) 50–55.
[6] P. Zwolak, A.Z. Dudek, Antineoplastic activity of zoledronic acid and denosumab, Anticancer Res. 33 (2013) 2981–2988.
[7] H.B. Sittig, Pathogenesis and bisphosphonate treatment of skeletal events and bone pain in metastatic cancer: focus on ibandronate, Onkologie 35 (2012) 380–387.
[8] L.L. Santos, T.B. Cavalcanti, F.A. Bandeira, Vascular effects of bisphosphonates-a systematic review, Clin. Med. Insights Endocrinol. Diabetes 5 (2012) 47–54.
[9] M. Okamoto, S. Yamanaka, W. Yoshimoto, T. Shigematsu, Alendronate as an effective treatment for bone loss and vascular calcification in kidney transplant recipients, J. Transplant. 2014 (2014) 269613.
[10] P.A. Price, S.A. Faus, M.K. Williamson, Bisphosphonates alendronate and ibandronate inhibit artery calcification at doses comparable to those that inhibit bone resorption, Arterioscler. Thromb. Vasc. Biol. 21 (2001) 817–824.
[11] R. Ross, Atherosclerosis–an inflammatory disease, N. Engl. J. Med. 340 (1999) 115–126.
[12] P. Libby, P.M. Ridker, A. Maseri, Inflammation and atherosclerosis, Circulation 105 (2002) 1135–1143.
[13] P.H. Cutini, V.L. Massheimer, Role of progesterone on the regulation of vascular muscle cells proliferation, migration and apoptosis, Steroids 75 (2010) 355–361.
[14] A.E. Campelo, P.H. Cutini, V.L. Massheimer, Cellular actions of testosterone in vascular cells: mechanism independent of aromatization to estradiol, Steroids 77 (2012) 1033–1040.
[15] P.H. Cutini, A.E. Campelo, V.L. Massheimer, Differential regulation of endothelium behavior by progesterone and medroxyprogesterone acetate, J. Endocrinol. 220 (2014) 179–193.
[16] Y. Kanno, T. Into, C.J. Lowenstein, K. Matsushita, Nitric oxide regulates vascular calcification by interfering with TGF-signalling, Cardiovasc. Res. 77 (2008) 221–230.
[17] N.L. D'Elía, A.N. Gravina, J.M. Ruso, J.A. Laiuppa, G.E. Santillán, P.V. Messina, Manipulating the bioactivity of hydroxyapatite nano-rods structured networks: effects on mineral coating morphology and growth kinetic, Biochim. Biophys. Acta 2013 (1830) 5014–5026.
[18] O.H. Lowry, N.J. Rosebrough, A.L. Farr, R.J. Randall, Protein measurement with the Folin phenol reagent, J. Biol. Chem. 193 (1951) 265–275.
[19] J. Mendiberri, M.B. Rauschemberger, J. Selles, V. Massheimer, Involvement of phosphoinositide-3-kinase and phospholipase C transduction systems in the nongenomic action of progesterone in vascular tissue, Int. J. Biochem. Cell Biol. 38 (2006) 288–296.
[20] M.J. Sandoval, P.H. Cutini, M.B. Rauschemberger, V.L. Massheimer, The soyabean isoflavone genistein modulates endothelial cell behaviour, Br. J. Nutr. 104 (2010) 171–179.
[21] A.E. Campelo, P.H. Cutini, V.L. Massheimer, Testosterone modulates platelet aggregation and endothelial cell growth through nitric oxide pathway, J. Endocrinol. 213 (2012) 77–87.
[22] P.H. Cutini, A.E. Campelo, E. Agriello, M.J. Sandoval, M.B. Rauschemberger, V.L. Massheimer, The role of sex steroids on cellular events involved in vascular disease, J. Steroid Biochem. Mol. Biol. 132 (2012) 322–330.
[23] A.R. Toledo-Piza, E. Nakano, R.E. Rici, D.A. Maria, Proliferation of fibroblasts and endothelial cells is enhanced by treatment with *Phyllocaulis boraceiensis* mucus, Cell Prolif. 46 (2013) 97–108.
[24] S. Viale-Bouroncle, M. Gosau, C. Morsczeck, Collagen I induces the expression of alkaline phosphatase and osteopontin via independent activations of FAK and ERK signalling pathways, Arch. Oral Biol. 59 (2014) 1249–1255.
[25] M.B. Rauschemberger, M.J. Sandoval, V.L. Massheimer, Cellular and molecular actions displayed by estrone on vascular endothelium, Mol. Cell. Endocrinol. 339 (2011) 136–143.
[26] K.A. Lomashvili, P. Garg, S. Narisawa, J.L. Millan, W.C. O'Neill, Upregulation of alkaline phosphatase and pyrophosphate hydrolysis: potential mechanism for uremic vascular calcification, Kidney Int. 73 (2008) 1024–1030.
[27] E.S. Park, J. Park, R.T. Franceschi, M. Jo, The role for runt related transcription factor 2 (RUNX2) as a transcriptional repressor in luteinizing granulosa cells, Mol. Cell. Endocrinol. 362 (2012) 165–175.
[28] M.P. Haynes, L. Li, K.S. Russell, J.R. Bender, Rapid vascular cell responses to estrogen and membrane receptors, Vasc. Pharmacol. 38 (2002) 99–108.
[29] T. Simoncini, P. Mannella, L. Fornari, A. Caruso, M.Y. Willis, S. Garibaldi, et al., Differential signal transduction of progesterone and medroxyprogesterone acetate in human endothelial cells, Endocrinology 145 (2004) 5745–5756.
[30] L.I. Plotkin, S.C. Manolagas, T. Bellido, Dissociation of the pro-apoptotic effects of bisphosphonates on osteoclasts from their anti-apoptotic effects on osteoblasts/osteocytes with novel analogs, Bone 39 (2006) 443–452.
[31] V. Ribeiro, M. Garcia, R. Oliveira, P.S. Gomes, B. Colaco, M.H. Fernandes, Bisphosphonates induce the osteogenic gene expression in co-cultured human endothelial and mesenchymal stem cells, J. Cell. Mol. Med. 18 (2014) 27–37.
[32] U. Forstermann, Nitric oxide and oxidative stress in vascular disease, Pflugers Arch. 459 (2010) 923–939.
[33] S.P. Duckles, V.M. Miller, Hormonal modulation of endothelial NO production, Pflugers Arch. 459 (2010) 841–851.
[34] L. Fu, T. Tang, Y. Miao, S. Zhang, Z. Qu, K. Dai, Stimulation of osteogenic differentiation and inhibition of adipogenic differentiation in bone marrow stromal cells by alendronate via ERK and JNK activation, Bone 43 (2008) 40–47.
[35] R.O. Silva, L.T. Lucetti, D.V. Wong, K.S. Aragao, E.M. Junior, P.M. Soares, et al., Alendronate induces gastric damage by reducing nitric oxide synthase expression and NO/cGMP/K(ATP) signaling pathway, Nitric Oxide 40 (2014) 22–30.
[36] N. Makkonen, A. Salminen, M.J. Rogers, J.C. Frith, A. Urtti, E. Azhayeva, et al., Contrasting effects of alendronate and clodronate on RAW 264 macrophages: the role of a bisphosphonate metabolite, Eur. J. Pharm. Sci. 8 (1999) 109–118.
[37] E.J. Dombrecht, A.J. Schuerwegh, C.H. Bridts, D.G. Ebo, J.F. Van Offel, W.J. Stevens, et al., Effect of bisphosphonates on nitric oxide production by inflammatory activated chondrocytes, Clin. Exp. Rheumatol. 25 (2007) 817–822.
[38] S.J. Wimalawansa, Nitric oxide and bone, Ann. N. Y. Acad. Sci. 1192 (2010) 391–403.
[39] S.J. Wimalawansa, Rationale for using nitric oxide donor therapy for prevention of bone loss and treatment of osteoporosis in humans, Ann. N. Y. Acad. Sci. 1117 (2007) 283–297.
[40] G. Misso, M. Porru, A. Stoppacciaro, M. Castellano, C.F. De, C. Leonetti, et al., Evaluation of the in vitro and in vivo antiangiogenic effects of denosumab and zoledronic acid, Cancer Biol. Ther. 13 (2012) 1491–1500.

[41] H.H. Mawardi, N.S. Treister, S.B. Woo, Bisphosphonate-Associated Osteonecrosis of the Jaws, in: C.J. Rosen (Ed.), Primer on the Metabolic Bone Diseases Disorders of Mineral Metabolism, Wiley-Blackwell, Ames 2013, pp. 929–940.
[42] L. Wu, L. Zhu, W.H. Shi, J. Zhang, D. Ma, B. Yu, Zoledronate inhibits the proliferation, adhesion and migration of vascular smooth muscle cells, Eur. J. Pharmacol. 602 (2009) 124–131.
[43] K.I. Bostrom, N.M. Rajamannan, D.A. Towler, The regulation of valvular and vascular sclerosis by osteogenic morphogens, Circ. Res. 109 (2011) 564–577.
[44] G. Pugliese, C. Iacobini, F.C. Blasetti, S. Menini, The dark and bright side of atherosclerotic calcification, Atherosclerosis 238 (2015) 220–230.
[45] D.A. Chistiakov, A.N. Orekhov, Y.V. Bobryshev, Vascular smooth muscle cell in atherosclerosis, Acta Physiol (Oxford) 214 (2015) 33–50.
[46] K. Mori, A. Shioi, S. Jono, Y. Nishizawa, H. Morii, Expression of matrix Gla protein (MGP) in an in vitro model of vascular calcification, FEBS Lett. 433 (1998) 19–22.
[47] H. Epstein, V. Berger, I. Levi, G. Eisenberg, N. Koroukhov, J. Gao, et al., Nanosuspensions of alendronate with gallium or gadolinium attenuate neointimal hyperplasia in rats, J. Control. Release 117 (2007) 322–332.
[48] Q. Li, J. Kingman, J.P. Sundberg, M.A. Levine, J. Uitto, Dual effects of bisphosphonates on ectopic skin and vascular soft tissue mineralization versus bone microarchitecture in a mouse model of generalized arterial calcification of infancy, J. Invest. Dermatol. 136 (2016) 275–283.